Laser-induced fluorescence measurement of plasma ion temperatures: Corrections for power saturation

M. J. Goeckner and J. Goree

Department of Physics and Astronomy, The University of Iowa, Iowa City, Iowa 52242-1479

When using high-power pulsed tunable dye lasers to measure plasma ion temperatures, it is important to attenuate the laser intensity. The temperature is found from the Doppler broadening of a spectral line. This may be obscured by saturation broadening, an instrumental effect encountered when too much laser intensity is used. Three useful experimental methods for determining the optimum pulsed laser intensity are found from a semiclassical atomic physics model. As an example, an Ar II transition pumped by a 1-GHz bandwidth laser is examined. The fluorescence linewidth of room-temperature ions broadens from 1.50 to 2.87 GHz when the homogeneous laser intensity is increased from 50 kW/m² to 5 MW/m².

I. INTRODUCTION

The correct measurement of low ion temperatures is an important and difficult task.[1] A reliable diagnostic will enable the accurate study of ion heating, ion acoustic waves, and related phenomena. These processes can be important in gas discharge, fusion, and other plasmas.[2]

Plasma ion energies are often measured with an *in situ* electrical device, an energy analyzer. The device has two major drawbacks. The first is the electrical nature of the energy analyzer. This will perturb the local plasma potential. The second drawback is possible contamination of the plasma by an *in situ* device. Contaminates may produce changes in the plasma characteristics and in the surface conditions.

An alternate method for measurement of ion energies is the use of laser-induced fluorescence (LIF).[2–4] LIF measurements do not disturb or contaminate the plasma. When nonperturbative ion measurements are necessary, as with processing plasmas, LIF is the logical diagnostic.

LIF is a relatively new plasma diagnostic technique.[5] While LIF can be used for a variety of measurements, we will only consider ion energies. This technique is possible because of the Doppler shift of a moving ion's absorption line. Ion distribution functions are determined by measuring the Doppler broadened spectral line shape.

Some recent studies using this technique have employed pulsed lasers.[2,6] Pulsed lasers are characterized by broad frequency bandwidth, 0.5–6 GHz, high intensity, 0.01–1.0 GW/m², and short pulse duration, 5–20 ns. They introduce instrumental broadening of the spectral line not found when cw lasers are used. Instrumental broadening must be minimized for accurate measurement of ion distribution functions.

One type of instrumental broadening, encountered with the use of high-intensity pulsed lasers, is the result of power saturation. Saturation occurs when the stimulated photon emission rate is equivalent to the photon absorption rate and greater than the spontaneous photon emission rate. Increases in laser intensity will not change this balance. When saturation occurs at frequencies in the wings of the laser line, the measured fluorescence line is broadened. This is known as saturation or power broadening.

Ignoring power broadening may result in measurement errors of the ion temperature. These errors can be several orders of magnitude. By reducing the laser intensity, this problem can be avoided. However, reducing the intensity diminishes the fluorescence signal. The balance of a strong signal and minimal instrumental broadening determines the most desirable laser intensity.

To see how laser intensity broadens the fluorescence linewidth, it is necessary to develop a basic model of LIF. This paper treats LIF as a semiclassical process in a collisionless plasma. Although a completely quantum-mechanical description of the photon–ion interaction was described by Glauber[7] and Mollow,[8–12] we chose to work with the semiclassical model for simplicity. Theoretical results for spatially homogeneous pulses of laser light are presented and discussed.

Three simple experimental methods for selecting the optimum laser intensity are given.

II. SEMICLASSICAL MODEL OF LIF

Fluorescence is produced in a simple manner. Laser light, tuned close to a specific transition of the ion, is directed through the plasma. Ions that absorb the laser photons can then decay via spontaneous emission to a lower state. These spontaneously emitted photons, i.e., fluorescence, constitute the LIF signal. The fluorescence line is examined by scanning the laser's frequency through the ion's transition. A number of phenomena, including Doppler broadening, collisional broadening, and saturation broadening, determine the fluorescence line shape.

Doppler broadening is a simple process. It arises from the Doppler shift, $2\pi\Delta\nu = k\cdot v$, of the absorption spectrum. If this were the only line broadening mechanism, a Maxwellian ion distribution would result in a linewidth characterized by the uncorrected frequency full width at half-maximum (FWHM) of

$$\text{FWHM}_{\text{unc}} = 2\nu_{01}\left(\frac{2T_i \ln 2}{m_i c^2}\right)^{1/2}, \quad (1)$$

where m_i is the ion mass, c is the speed of light, T_i is the ion

temperature in units of energy, and ν_{01} is the central frequency of the transition. While this equation offers an easy method for determining the ion temperature, we will show it can be incorrect.

Collisional broadening of the fluorescence line has been well studied.[13] Our equations will at first include source terms in which collisional transitions could be accounted for, but these terms are assumed to be small and will be dropped from the final analysis.

Saturation or power broadening is caused by multiple processes. They are absorption, stimulated emission, and spontaneous emission of photons. This broadening can be understood by examining how these processes change the population densities of three states of an ion, denoted 0, 1, and 2. The laser is tuned near the $0 \rightarrow 1$ transition while an ion decaying via the $1 \rightarrow 2$ transition produces a fluorescence photon. This is shown in Fig. 1.

Absorption occurs when an ion in state i interacts with a photon near the transition frequency ν_{ij}. This causes an upward transition from state i to state j. Single ions, with a velocity component v along the laser beam, have a normalized probability $(B_{ij}/4\pi)L(\nu,\nu_{ij},v)\,dv\,dt$ of absorbing a single photon with frequency from v to $v + dv$ in time dt. The proportionality constant B_{ij} is the Einstein absorption coefficient defined for light of isotropic intensity. Multiplying by the intensity frequency spectrum, $I(x,v,t)$, and the density of ions of velocity v, $f_i(x,v,t)$, gives the number of these transitions occurring in time dt. Integrating over frequency gives the rates of change, produced by absorption, for the densities of states i and j,

$$-\frac{d}{dt}f_i(x,v,t) = \frac{d}{dt}f_j(x,v,t)$$

$$= f_i(x,v,t)\frac{B_{ij}}{4\pi}\int_0^{+\infty} dv\,L(v,\nu_{ij},v)I(x,v,t)\ .$$

Stimulated emission occurs when an ion in state j interacts with a photon near the transition frequency ν_{ij}. This causes a downward transition from state j to state i. In the semiclassical model the interaction probability is the same as that of absorption, $L(v,\nu_{ij},v)dv\,dt$.[14] This process changes the den-
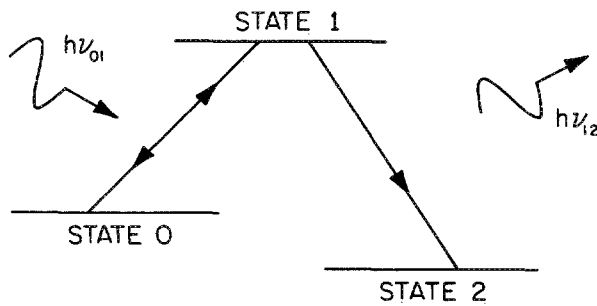

FIG. 1. The laser-induced fluorescence process. Ions are pumped from state 0 to state 1. The ions in state 1 then have a probability of spontaneously decaying into state 2. Photons produced by this spontaneous transition comprise the fluorescence signal. The strength of this signal is determined by density of ions in state 1. The mechanisms changing the density of state 1 are stimulated and spontaneous photon emission by ions in state 1 and photon absorption by ions in state 0.

sities of states i and j at the rates

$$\frac{d}{dt}f_i(x,v,t) = -\frac{d}{dt}f_j(x,v,t)$$

$$= f_j(x,v,t)\frac{B_{ji}}{4\pi}\int_0^{+\infty} dv\,L(v,\nu_{ij},v)I(x,v,t)\ ,$$

where B_{ji} is the Einstein stimulated emission coefficient defined for light of isotropic intensity.

Spontaneous emission occurs without the presence of external photons. This decay is a downward transition from state j to state i. The density of state i changes at the rate

$$\frac{d}{dt}f_i(x,v,t) = A_{ji}f_j(x,v,t)\ ,$$

where A_{ji} is the Einstein spontaneous emission coefficient. The sum of all these spontaneous decay rates is the decay rate for state j

$$\frac{d}{dt}f_j(x,v,t) = -\sum_i A_{ji}f_j(x,v,t)$$

$$= -f_j(x,v,t)/\tau_j\ ,$$

where the $1/e$ time of state j is denoted by τ_j.

Other processes, unrelated to the laser light, can change the density of a state. They include ion–ion collisions, electron–ion collisions, and spontaneous emission from other upper states. These will be included in a single source term, $S_i(x,v,t)$, for each state.

Combining these processes we develop rate equations for the ion distribution functions of each of the ion states. The set of rate equations[14] for states 0, 1, and 2 are

$$\frac{d}{dt}f_0(x,v,t) = S_0(x,v,t) + f_1(x,v,t)\,[A_{10} + B_{10}\Phi(x,v,t)]$$

$$- f_0(x,v,t)\left(\frac{1}{\tau_0} + B_{01}\Phi(x,v,t)\right),\qquad (2)$$

$$\frac{d}{dt}f_1(x,v,t) = S_1 + f_0(x,v,t)B_{01}\Phi(x,v,t)$$

$$- f_1(x,v,t)\left(\frac{1}{\tau_1} + B_{10}\Phi(x,v,t)\right),\qquad (3)$$

$$\frac{d}{dt}f_2(x,v,t) = S_2(x,v,t) + A_{12}f_1(x,v,t)$$

$$- (\tau_2)^{-1}f_2(x,v,t)\ ,\qquad (4)$$

where

$$\Phi(x,v,t) = \frac{1}{4\pi}\int_0^{+\infty} dv\,L(v,\nu_{ij},v)I(x,v,t)$$

is an effective isotropic laser intensity. This is the complete set of empirical rate equations governing the LIF process. To use these equations the laser intensity spectrum, $I(x,v,t)$, the ion absorption spectrum, $L(v,\nu_{ij},v)$, and the ion distribution functions, $f_i(x,v,t)$, must be specified.

Lasers do not have a monochromatic intensity spectrum. They emit a frequency spectrum dependent upon the physical characteristics of the laser cavity and lasing medium. Because these characteristics vary from laser to laser, the power spectrum varies from laser to laser. A simple model of the laser beam employs a Gaussian frequency distribution

$$I(x,v,t) = I_0\theta(t)\xi(x)\left(\frac{4\ln 2}{\pi}\right)^{1/2}(\delta v_i)^{-1}$$

$$\times \exp\left[4\ln 2\left(\frac{v-v_i}{\delta v_i}\right)^2\right]$$

with $\theta(t)$ a dimensionless temporal dependence, $\xi(x)$ a dimensionless spatial dependence, v the frequency, v_i the central frequency, and δv_i the bandwidth. Experimenters

$$I(x,v,t) = \begin{cases} I_0[4\ln 2/\pi(\delta v_1)^2]^{1/2}\exp\{4\ln 2[(v-v_1)/\delta v_1]^2\} & 0\leqslant t \leqslant T \\ 0 & \text{otherwise} \end{cases}$$

is our model of the laser intensity.

The classical photon absorption spectrum is derived by modeling a motionless ion as a driven harmonic oscillator.[14] For light of frequency v, near the transition v_{ij}, this model gives a Lorentzian absorption probability. Thus

$$L(v,v_{ij},v=0) = \frac{A_{ji}/\pi}{[(v-v_{ij})^2 + A_{ji}^2]},$$

where A_{ji} is the decay rate from state j to state i. When the Doppler shift is included, the absorption curve for an ion with velocity $\mathbf{v}$ in the laboratory rest frame becomes

$$L(v,v_{ij},v) = \frac{A_{ji}/\pi}{\{[v-v_{ij}(1+v/c)]^2 + A_{ji}^2\}},$$

where v is the component of the ion velocity parallel to the laser beam.

The ion distribution functions are assumed to be homogeneous Maxwellians,

$$f_k(x,v) = n_k\left(\frac{m_i}{2\pi T_i}\right)^{1/2}\exp\left(-\frac{m_i v^2}{2T_i}\right),$$

where k represents the atomic state and n_k the state's spatial density. Before the laser is turned on at time $t=0$, each state has the same form:

$$f_0(x,v,t\leqslant 0) = n_0\left(\frac{m_i}{2\pi T_i}\right)^{1/2}\exp\left(-\frac{m_i v^2}{2T_i}\right),$$

$$f_1(x,v,t\leqslant 0) = n_1\left(\frac{m_i}{2\pi T_i}\right)^{1/2}\exp\left(-\frac{m_i v^2}{2T_i}\right),$$

should characterize their laser. If the laser has a different power spectrum, the following equations should be reevaluated.

Spatial dependence will be treated in a future paper. Presently the beam is assumed to be uniform. Temporal dependence may vary from shot to shot. To keep the model as simple as possible, $\theta(t)$ is assumed to be unity during the laser pulse, $0\leqslant t \leqslant T$, and zero otherwise. Thus

$$f_2(x,v,t\leqslant 0) = n_2\left(\frac{m_i}{2\pi T_i}\right)^{1/2}\exp\left(-\frac{m_i v^2}{2T_i}\right).$$

To obtain a large signal the experimenter must choose a state 0 with a long lifetime and a state 1 with a short lifetime. This gives state 0 a large initial density and state 1 a small initial density. Thus

$$n_0 \gg n_1 . \tag{5}$$

With this semiclassical model of LIF, theoretical calculations of the fluorescence signal can be performed. By examining how the laser intensity distorts the signal, methods are found to determine the optimum intensity for use of LIF as a diagnostic tool.

III. RESULTS

The LIF signal comes from detecting the photon emitted as an ion decays from state 1 to state 2. The number of fluorescence photons collected is

$$N_{\text{obs}} = \frac{d\Omega}{4\pi}A_{12}\int d^3x \int d^3v \int_0^{+\infty} dt\, f_1(x,v,t) ,$$

where $d\Omega$ is the detector's solid angle. Solving the coupled rate equations, Eqs. (2)–(4), using the assumption that the external source terms S_i are small, and integrating over time yields

$$N_{\text{obs}} = \frac{d\Omega}{4\pi}A_{12}\int d^3x \int d^3v f_0(x,v,t=0)B_{10}\Phi(x,v)(\Gamma\chi)^{-1}\left(4\Gamma^{-1} - \{2\Gamma^{-1}[1+(1-\chi)^{-1/2}] - \tau_1\chi(1-\chi)^{-1/2}\}\right.$$

$$\times \exp\left\{-\frac{T}{2}\Gamma[1-(1-\chi)^{-1/2}]\right\} + \{2\Gamma^{-1}[1-(1-\chi)^{-1/2}] - \tau_1\chi(1-\chi)^{-1/2}\}$$

$$\left.\times \exp\left\{-\frac{T}{2}\Gamma[1+(1-\chi)^{-1/2}]\right\}\right), \tag{6}$$

where we have defined

$$\Gamma(x,v) = \left(\frac{1}{\tau_0} + \frac{1}{\tau_1} + (B_{01} + B_{10})\Phi(x,v)\right)$$

and

$$\chi(x,v) = \frac{4}{\Gamma^2}\left[\frac{1}{\tau_0\tau_1} + \Phi(x,v)\left(B_{01}(\tau_1^{-1} - A_{10}) + \frac{B_{10}}{\tau_0}\right)\right].$$

When state 0 and state 2 are identical, A_{10} will replace A_{12} in Eq. (6).

TABLE I. The parameters used for Figs. 2–4. This corresponds to probing the Ar II transition, $3d'^2G_{9/2} \to 4p'^2F^0_{7/2} \to 4s'^2D_{5/2}$, with a typical broad bandwidth high-intensity pulsed laser.

Parameter	Value	Units	Reference
δv_1	1.0	GHz	
λ_0	611.492	nm	[15]
A_{10}	0.212	$10^8\,\mathrm{s}^{-1}$	[16]
A_{12}	0.759	$10^8\,\mathrm{s}^{-1}$	[16]
B_{10}	121.9	$10^{11}\,\mathrm{m}^2(\mathrm{J\,s})^{-1}$	
B_{01}	97.55	$10^{11}\,\mathrm{m}^2(\mathrm{J\,s})^{-1}$	
τ_1	8.51	ns	
τ_0	$\geqslant 1.0$	ms	
T	17.0	ns	
m_i	39.962	amu	

To determine the linewidth, Eq. (6) is calculated numerically. By plotting N_{obs} versus the laser frequency, we arrive at our theoretical prediction of the line shape. As an example, we examined the Ar II transition $3d'^2G_{9/2} \leftrightarrow 4p'^2F^0_{7/2} \to 4s'^2D_{5/2}$. This transition was used by Anderegg et al.[2] to observe ion heating. They employed a laser with a bandwidth δv_l of 1 GHz and a pulse duration T of 17 ns. These parameters were used in our computation; a list is provided in Table I.

Figure 2 shows the fluorescence FWHM as a function of ion temperature. The correct linewidths are found by computing Eq. (6) for a set of laser frequencies near the transition frequency of a motionless ion. They are compared to the uncorrected linewidth found from Eq. (1). The fluorescence line is broadened by high laser intensities. When this broadening occurs, Eq. (1) will not provide the correct ion temperature.

Figure 3 shows the fluorescence FWHM as a function of laser intensity. If the laser intensity is increased above a certain level, saturation broadening occurs. Below this level, the fluorescence linewidth has little variation.

FIG. 3. The LIF frequency linewidth as a function of laser intensity for various ion temperatures. Saturation broadening occurs for large intensities. The laser intensity can be optimized by producing this curve experimentally and finding the slope of the tangents, σ. The intensity is chosen to be optimum when $\sigma = 0.015$. Laser intensities above the optimum will broaden the fluorescence linewidth.

Figure 4 shows the fraction of ions, as a function of laser intensity, that make the $0 \to 1 \to 2$ transition when the laser is tuned to v_{01}. This is a measure of the relative signal level. The signal diminishes proportional to the intensity when the laser power is weak. Above a certain laser intensity, the signal strength reaches an asymptotic limit. This asymptotic limit is caused by the saturation of the $0 \to 1$ transition.

Optimizing the laser intensity requires the balance of a strong fluorescence signal with minimal saturation broadening. Three arbitrary methods for choosing the optimum intensity are suggested by an examination of Figs. 2 to 4.

The first experimental method for optimizing the laser intensity is inferred from Fig. 2. As the laser intensity is
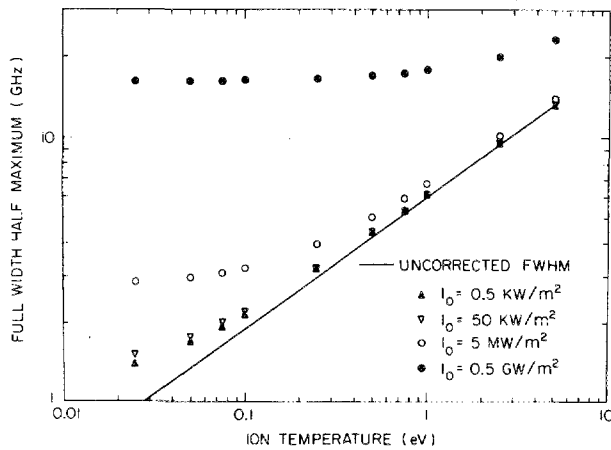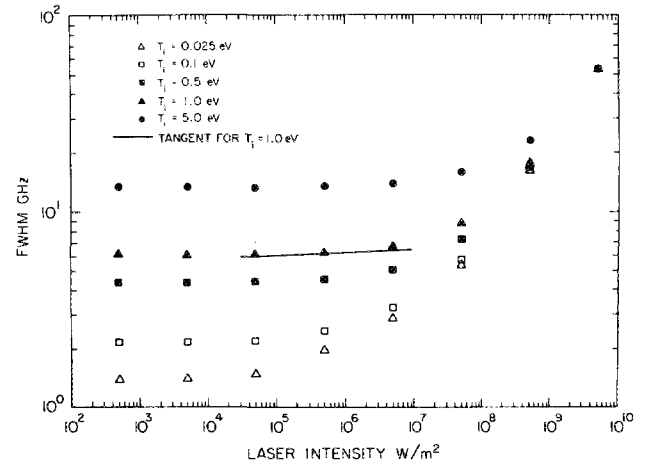

FIG. 2. The LIF frequency linewidth as a function of ion temperature for various laser intensities. The solid line represents a fluorescence linewidth that is uncorrected for all broadening mechanisms except Doppler broadening. As the homogeneous laser intensity is lowered, this uncorrected linewidth becomes a better approximation. Lowering the laser intensity below a certain level produces little change in the fluorescence linewidth.
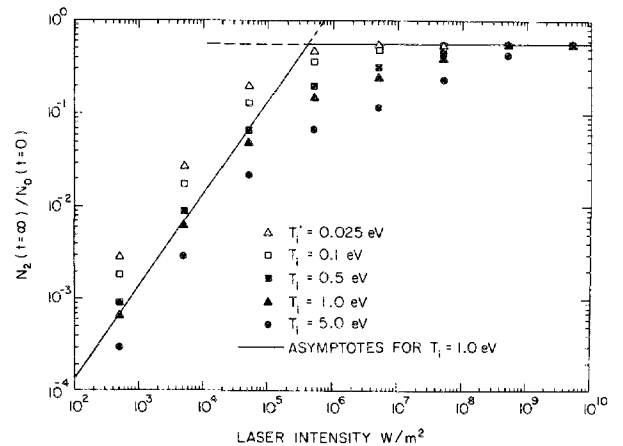

FIG. 4. The fraction of ions that produce fluorescence photons when the laser frequency is tuned to maximize the signal. Saturation broadening occurs when a large fraction of all ions produce fluorescence. The laser power levels can be optimized by determining the asymptotes of the signal strength for high and low intensities. The optimum is one-half the intensity at which these lines cross. An alternate method of optimizing the laser is to decrease the intensity until the fluorescence signal is one-fifth of the maximum. Laser intensities below the optimum will simply reduce the signal strength.

lowered, the FWHM of the fluorescence curve will approach the value found by Eq. (1). The experimenter measures the fluorescence FWHM as a function of the intensity, while the plasma parameters remain constant. Plotting the measured data on log–log graphs will result in curves as shown in Fig. 3. The tangent of the experimental curve will be of the form

$$\log_{10}(\text{FWHM}) = \sigma \log_{10} I + \text{constant},$$

where σ is the slope. The laser intensity is chosen to be optimum when $\sigma = 0.015$. Curve-fitting algorithms, such as a cubic spline fit, can determine slopes. Figure 4 shows that decreasing the intensity below the optimum value will decrease the signal strength, and Fig. 3 shows that increasing the intensity broadens the fluorescence line. In Fig. 3 the optimum intensity for $T_i = 1.0$ eV is 500 kW/m^2.

The second experimental method for optimizing the laser intensity is inferred from Fig. 4. The relative LIF signal, when the laser is tuned to ν_{01}, becomes asymptotic at high and at low laser intensities. The optimum laser intensity is one-half the intensity at which the asymptotes intersect. Intensities below this value will decrease signal strength and intensities above it will broaden the fluorescence line. In Fig. 4 the asymptotes for $T_i = 1.0$ eV intersect at $I = 500$ kW/m^2. Thus the optimum laser intensity is 250 kW/m^2. This compares well with the optimum found by the first method.

The third experimental method for optimizing the laser intensity is also inferred from Fig. 4. The experimenter tunes the laser to find the maximum signal strength. The laser intensity is then diminished until the fluorescence signal is reduced by a factor of 5. For $T_i = 1.0$ eV this optimum intensity is 190 kW/m^2. This intensity is close to those found by the other methods.

Note that the results presented above are for a laser frequency bandwidth of 1 GHz. By selecting a laser with a narrower bandwidth, which produces less instrumental broadening, lower temperatures can be measured more accurately. Likewise, using a laser with a wider bandwidth will result in more instrumental broadening and less accuracy.

IV. CONCLUSIONS

Large errors in the measured ion temperatures result from neglecting instrumental broadening, including saturation broadening. Saturation occurs when the laser intensity is high enough that the $0 \rightarrow 1$ photon absorption and $1 \rightarrow 0$ stimulated emission rates are approximately equal and large

compared to the $1 \rightarrow 0$ spontaneous emission rate,

$$f_0(x,v,t)B_{01}\Phi(x,v,t) \approx f_1(x,v,t)B_{10}\Phi(x,v,t) > A_{10}f_1(x,v,t).$$

If the laser intensity is lower than this, saturation and saturation broadening will be minimized. Saturation broadening can be seen in Figs. 2 and 3. Saturation can be seen in Fig. 4.

Optimal laser intensities, which balance a strong signal with minimal saturation broadening, can be determined experimentally. They are chosen so that very weak saturation occurs. This assures a relatively strong fluorescence signal but minimal power broadening. The three arbitrary methods, discussed above, involve either measuring the fluorescence frequency bandwidth or the signal strength as a function of the laser intensity.

ACKNOWLEDGMENTS

[1]N. D'Angelo and M. J. Alport, Plasma Phys. 24, 1291 (1982).
[2]F. Anderegg, R. A. Stern, B. A. Hammel, M. Q. Tran, P. J. Paris, and P. Kohler, Phys. Rev. Lett. 57, 329 (1986), and references therein.
[3]R. A. Gottscho and T. A. Miller, Pure Appl. Chem. 56, 189 (1984), and references therein.
[4]T. A. Miller, J. Vac. Sci. Technol. A 4, 1768 (1986), and references therein.
[5]R. A. Stern and J. A. Johnson, Phys. Rev. Lett. 24, 1548 (1975).
[6]J. M. McChesney, R. A. Stern, and P. M. Bellan, Phys. Rev. Lett. 59, 1436 (1987).
[7]R. J. Glauber, Phys. Rev. 130, 2529 (1963).
[8]B. R. Mollow, Phys. Rev. 188, 1969 (1969).
[9]B. R. Mollow, Phys. Rev. A 2, 76 (1970).
[10]B. R. Mollow, Phys. Rev. A 5, 1522 (1972).
[11]B. R. Mollow, Phys. Rev. A 8, 1949 (1973).
[12]B. R. Mollow, Phys. Rev. A 15, 1023 (1977).
[13]H. R. Griem, Spectral Line Broadening by Plasmas (Academic, New York, 1974).
[14]A. Corney, Atomic and Laser Spectroscopy (Oxford University, New York, 1977).
[15]G. Nolén, Phys. Scr. 8, 249 (1973).
[16]G. García and J. Campos, J. Quant. Spectrosc. Radiat. Transfer 34, 85 (1985).